

Influence of Diode Reverse Recovery on the Operation and Design of High-Frequency Rectifiers

Lupco V. Karadzinov

Faculty of Electrical Engineering,
St. Cyril and Methodius University,
Karpos II b.b., P.O.Box 574, 91000 Skopje, Macedonia,
tel. +389 91 363566, fax +389 91 364262,
e-mail: L.Karadzinov@ieee.org

David C. Hamill

Surrey Space Centre, University of Surrey,
Guildford, Surrey GU2 5XH, England,
tel.+44 1483 300800, fax +44 1483 534139,
e-mail: D.Hamill@surrey.ac.uk

Abstract — Diode reverse recovery can cause anomalies in high-frequency rectifier operation, including self-sustaining quasiperiodic oscillations. The output voltage can increase considerably beyond that predicted by the usual analysis. This nonlinear effect is analysed using a recently developed piecewise-linear diode model. The theoretical results are confirmed by experiment. Design guidelines are presented to avoid overvoltage and instability in practical converters.

1. INTRODUCTION

PWM and resonant switching converters operating at high switching frequencies have complex voltage and current waveforms. This necessitates the use of many approximations in their analysis [1–4]. The most common is the use of ideal switches as models for the semiconductor devices. For resonant converters, to further simplify the analysis and design, the fundamental-component method is frequently used [3, 5]. This gives good results when the loaded Q factor is high and the switching frequency is close to the resonant frequency. However, such an analysis cannot predict all effects, some of which can cause the practical circuit to exhibit unexpected and sometimes strange behaviour.

In this paper we are concerned with the phenomenon of increased output voltage in a high-frequency bridge rectifier fed by an inductive source, as shown in Fig. 1. This rectifier (or similar) forms part of many power converters. The inductance can be introduced intentionally, or it can come from leakage

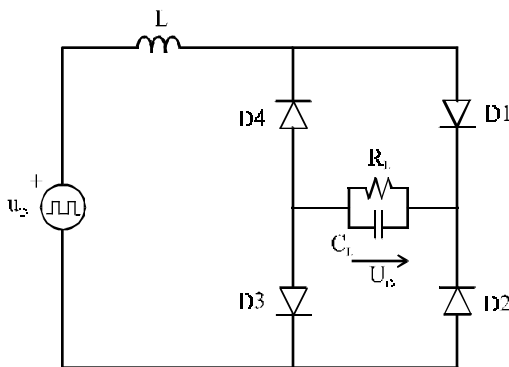


Fig. 1. Class D bridge rectifier with inductive drive

and stray inductances. In particular, it forms an essential part of the series-resonant converter, Fig. 2, where this effect was first noticed [6]. Analysing these converters using ideal switches, explicit equations can be obtained for the output voltage V_O . According to these equations, the output voltage is always lower than the input drive voltage [3, 5]. However, in practical converters with certain circuit parameters, e.g. when the rectifier circuit employs slow power diodes or has light loading, there are considerable deviations from ideal operation.

These deviations are clearly depicted in Fig. 3, which shows how the measured output voltage depends on the drive frequency. Fig. 3 uses the series-resonant converter model of Fig. 4 with the following parameters: $V_{Dpk-pk} = 10$ V, $L = 9.42$ mH, $C = 23.2$ nF, four diodes MR752 with storage delay time

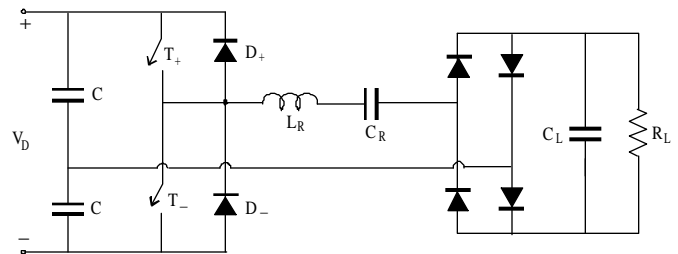


Fig. 2. Series-resonant converter (SRC)

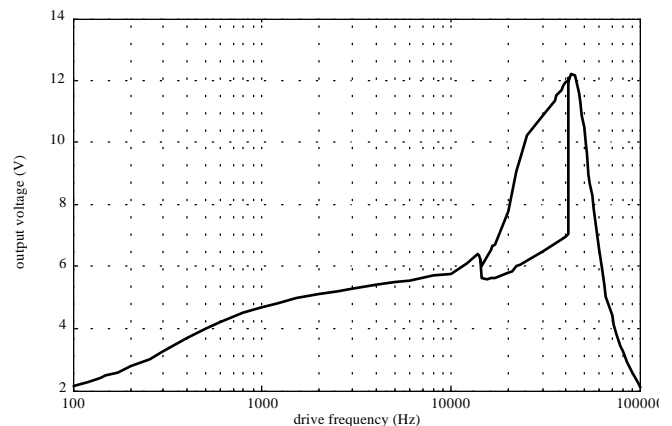


Fig. 3. Measured deviations from ideal operation of the SRC. The output voltage is considerably higher than that predicted by analysis. From 14 kHz to 41 kHz, the output voltage oscillates between two levels.

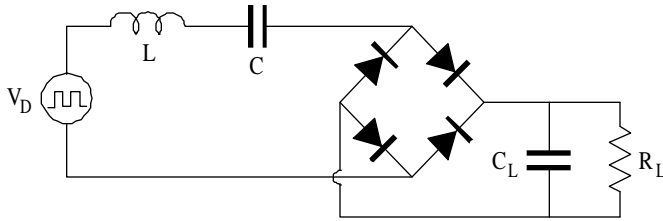


Fig. 4. Model of the series-resonant converter

$t_{sd} = 5 \mu\text{s}$ ($\tau = 7.2 \mu\text{s}$), $C_L = 61.5 \text{ nF}$ and load $R_L = 10 \text{ k}\Omega$. Above the resonant frequency $f_0 = 10.766 \text{ kHz}$, the output voltage rises. At 45 kHz it reaches its maximum: 2.4 times that predicted by analysis, $V_{Dpk-pk}/2$. At frequencies below the maximum, the output voltage oscillates between two levels, depicted by two lines in Fig. 3.

This oscillation was first described by Deane and Hamill [6] and was subsequently named the *DH phenomenon* [8, 9]. Fig. 5 shows the bridge rectifier's input voltage. This square-wave voltage appears amplitude-modulated at a frequency apparently unrelated to the switching frequency (quasi-periodicity). The output voltage follows the envelope of the bridge voltage and thus has the same modulation. This might cause the converter to malfunction, especially if it enters a control loop.

The above behavior is quite robust: it exists for a wide range of circuit parameters and with different diode types. For example, computer simulations of the DH phenomenon [7, 9] show that it depends only slightly on the capacitance C in the series resonant circuit. Even if C is absent, i.e. if we have the circuit of Fig. 1, the phenomenon is present in the circuit with its full complexity, as shown in Fig. 6. The only difference is that the voltage dependence on frequency is flat below resonance. Deane and Hamill [6] found that this behaviour is caused by the diodes' nonlinear transient characteristics, e.g. reverse recovery. Similar effects occur frequently in practice, but they are rarely reported in the literature and, to the best of our knowledge, no analysis has been presented to date.

In this paper we analyse the influence of reverse recovery on the operation of bridge rectifiers, and determine design constraints to prevent these effects. Until recently, the main

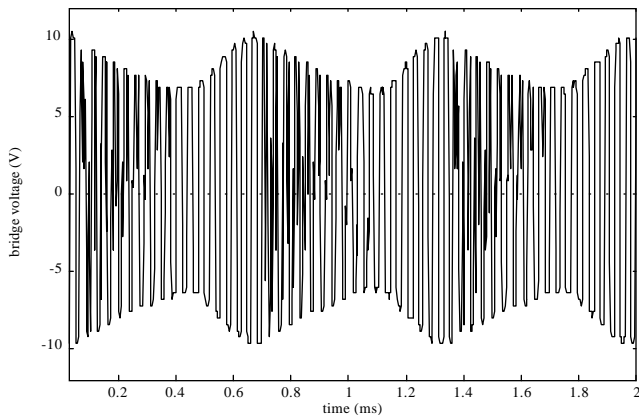


Fig. 5. DH phenomenon in series-resonant converter: case when $f = 27 \text{ kHz}$

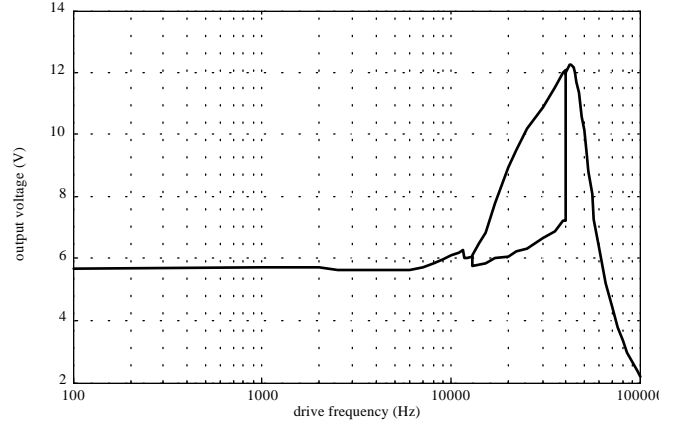


Fig. 6. Measured output voltage dependence on the drive frequency in the circuit of Fig. 1

obstacle to analysis has been the lack of an appropriate diode model: one that is not only simple enough to allow analysis but is also accurate enough to reveal the observed phenomena. Recently, however, a suitable piecewise-linear (PWL) diode model has been developed [8]. This model, used in our analysis, is shown in Fig. 7. It comprises two linear capacitances, a linear resistance, and an ideal switch, whose state depends on the anode-cathode voltage. The PWL model is capable of modeling, to first order, transient effects such as reverse recovery.

2. IDEAL OPERATION

For comparison purposes, we first analyse ideal operation of the rectifier in Fig. 1. The filter capacitor C_L at the output is assumed to be very large, as normal in applications requiring a nearly constant instantaneous output voltage $v_o \approx V_o$. The drive voltage v_D is a square wave with amplitude $\pm V_D$ and period T . The diodes are modelled initially as ideal switches which turn on and off instantaneously.

Inductor current i_L and voltage v_L waveforms are shown in Fig. 8. Under steady-state conditions, these waveforms are symmetrical with respect to zero and have equal peak values $|I_{LMAX}| = |I_{LMIN}|$ (i.e. area A is equal to area B). This gives:

$$\frac{V_D + V_o}{L} \cdot T_1 = \frac{V_D - V_o}{L} \cdot \left(\frac{T}{2} - T_1 \right)$$

This equation has two unknowns, V_o and T_1 . The second equation needed for determining these unknowns is obtained from the output stage of the converter:

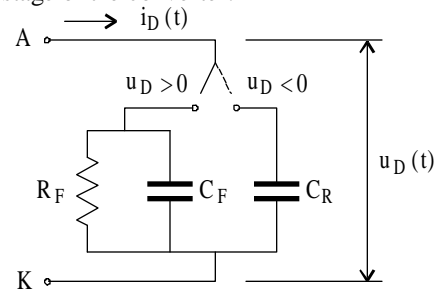


Fig. 7. Simplest PWL diode model exhibiting transient behavior.

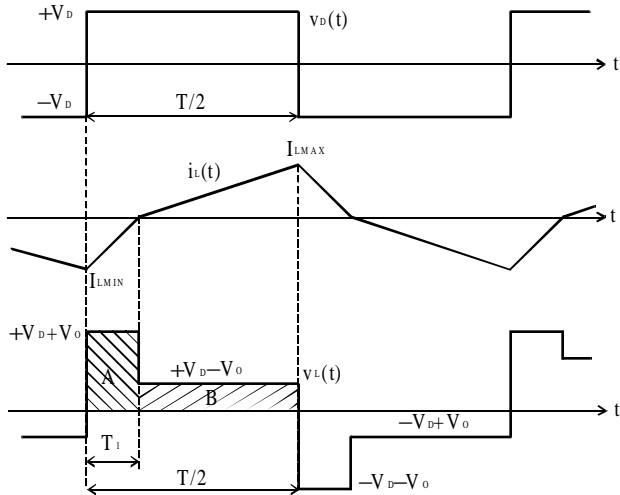


Fig. 8. Ideal operation of the rectifier in Fig. 1: drive, inductor current and voltage waveforms

$$V_o = R_L \cdot I_o = R_L \cdot \frac{I_{LMAX}}{2}$$

where

$$I_{LMAX} = \frac{V_D + V_o}{L} \cdot T_1$$

After some algebra, we obtain the following expressions in V_o and T_1 :

$$\frac{V_o}{V_D} = -\frac{4L}{R_L T} + \sqrt{\left(\frac{4L}{R_L T}\right)^2 + 1} \quad (1)$$

$$T_1 = \frac{2L}{R_L} \cdot \frac{V_o / V_D}{V_o / V_D + 1} \quad (2)$$

Equation (1) shows that at a given inductance value, the normalized output voltage depends on the drive frequency ($1/T$) and the load. Figs. 9 and 10 show a family of curves for a range of parameter $a = 4L/R_L$. Fig. 9 shows that output voltage is never greater than V_D . Each curve has a value of a ten times larger than the adjacent curve, shifting it a decade higher in frequency. This is obvious from the equation as well.

Fig. 10 shows that the pulses' delay time T_1 is nearly constant for low frequencies, and is equal to the circuit time con-

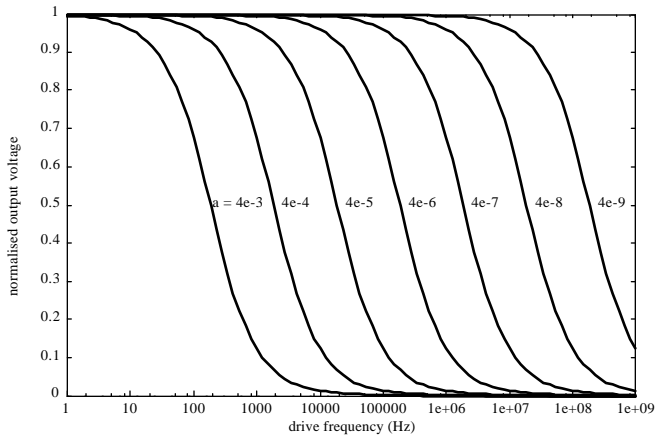


Fig. 9. Output voltage dependence on frequency for a wide range of parameter $a = 4L/R_L$

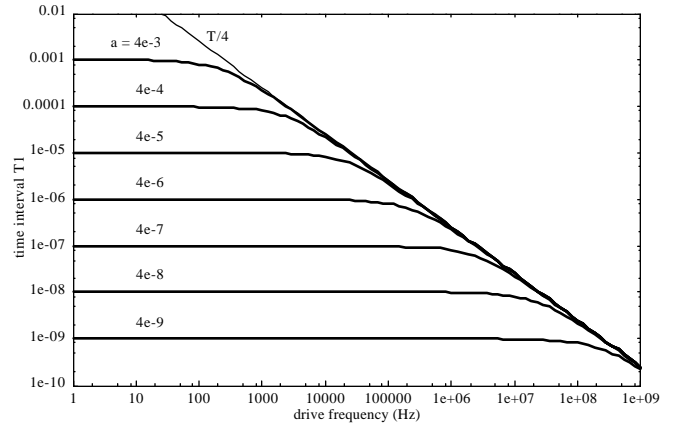


Fig. 10. Dependence on frequency of bridge pulses' delay time T_1 , for a wide range of parameter $a = 4L/R_L$

stant $\tau_L = L/R_L$. At high frequencies, T_1 decreases and approaches $T/4$.

3. OPERATION INCLUDING DIODE REVERSE RECOVERY

Next we analyse the circuit again, under the same assumptions as the ideal case but employing the PWL diode model of Fig. 7 instead of ideal diodes. Fig. 11 shows a model of the converter with D_1 and D_3 conducting. The diode forward voltages v_{D1} and v_{D3} are neglected in comparison with other circuit voltages v_D , v_L and v_o . As expected, the voltage and current waveforms (Fig. 12) show that the diodes do not switch off when the inductor current becomes negative at $t = T_1$. They conduct for an additional interval ΔT needed for stored excess minority charge carriers to be removed from the diode (reverse recovery). The delay time of the bridge pulses is now equal to the total diode conduction period $T_2 = T_1 + \Delta T$. To determine the steady-state output voltage, we need a system of three equations with three unknowns: either V_o , T_1 and ΔT , or V_o , T_2 and ΔT .

A. Qualitative Analysis

During the interval ΔT , negative current i_o flows through the output, discharging C_L (see area A_3 in Fig. 12(e)). In the ideal case discussed in the Section 2, the output current i_o was

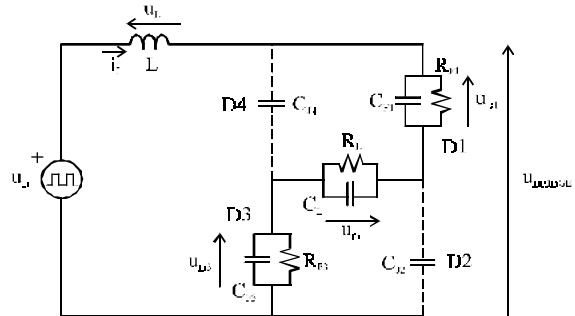


Fig. 11. Converter model with D_1 and D_3 conducting

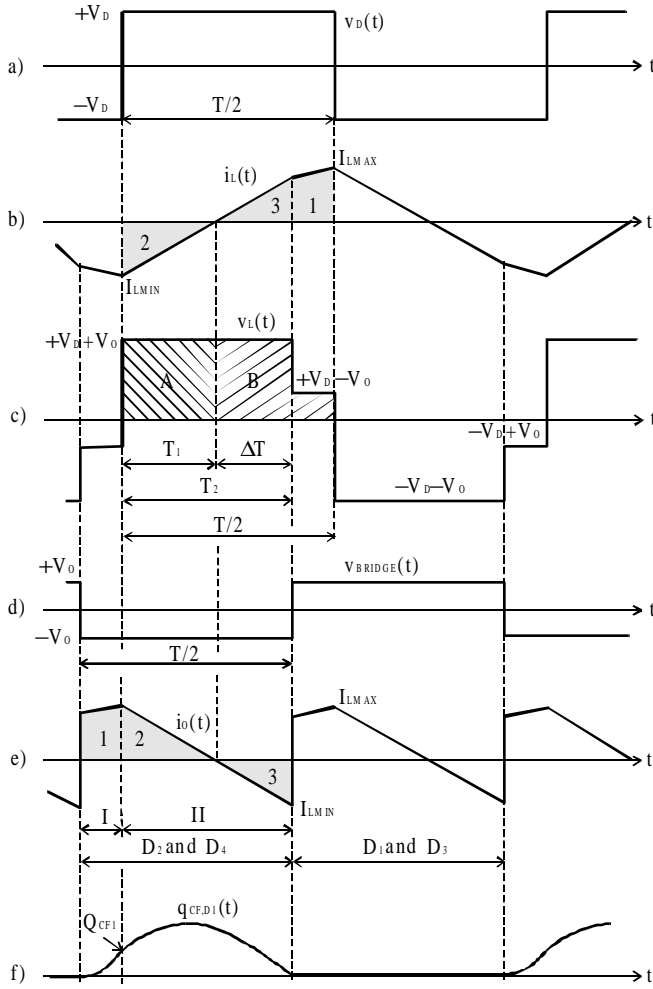


Fig. 12. Operation including diode reverse recovery (case when V_O is lower than V_D): (a) drive voltage, (b) inductor current, (c) inductor voltage, (d) bridge voltage, (e) diodes' and output current, and (f) charge on diode-model capacitance C_F .

always positive. But now the negative part, area A_3 , lowers the average output current value. By equating the energy drawn from the drive source to that delivered to the load, we see that the output voltage must be higher with reverse recovery than in the ideal case (assuming the same drive frequency).

A rough comparison can be made by looking at the shaded areas under the current waveforms of Fig. 12. Currents $I_{D(\text{half-cycle})}$ and I_O are proportional to the sum of the corresponding shaded areas: $I_{D(\text{half-cycle})} = 1/T (A_1 - A_2 + A_3)$ and $I_O = 1/T (A_1 + A_2 - A_3)$. Current I_O is larger than $I_{D(\text{half-cycle})}$ if $A_1 + A_2 - A_3 > A_1 - A_2 + A_3$, i.e. if $A_2 > A_3$.

Since these two areas are similar right-angled triangles, A_2 will be greater than A_3 if T_1 is greater than ΔT . When $\Delta T = T_1$, the two currents are the same, and $V_O = V_D$; when $\Delta T > T_1$, I_O is less than $I_{D(\text{half-cycle})}$ and $V_O > V_D$. This explains the effect, perhaps surprising at first encounter, that diode reverse recovery increases the output voltage.

B. Quantitative Analysis

Unlike the ideal case, here, three equations are needed to determine the three unknowns in the steady state. The first two equations can be obtained in a similar manner as before. First, the symmetry of the waveforms about the time axis (see Fig. 12) makes $|i_L|$ at the end of each half-cycle equal:

$$\frac{V_D + V_O}{L} \cdot T_1 = \frac{V_D + V_O}{L} \cdot \Delta T + \frac{V_D - V_O}{L} \cdot \left(\frac{T}{2} - T_1 - \Delta T \right)$$

$$\text{or} \quad \frac{V_D + V_O}{L} \cdot (T_2 - 2 \cdot \Delta T) = \frac{V_D - V_O}{L} \cdot \left(\frac{T}{2} - T_2 \right) \quad (3)$$

The output stage gives the second equation:

$$V_O = R_L \cdot I_O$$

where the current I_O can be obtained by averaging the diodes' current i_D :

$$I_O = \frac{1}{T/2} \int_0^{T/2} i_D d\tau = \frac{1}{T/2} \int_0^{T_2} \left(-\frac{V_D + V_O}{L} \tau + \frac{V_D + V_O}{L} T_1 \right) d\tau + \int_{T_2}^{T/2} \left(\frac{V_D - V_O}{L} (\tau - T_2) + \frac{V_D + V_O}{L} \Delta T \right) d\tau$$

Solving the integrals and using (3) we obtain:

$$I_O = \frac{V_D + V_O}{L} \cdot \frac{T_2}{T} \left(\frac{T}{2} - 2\Delta T \right)$$

$$\text{or} \quad V_O = R_L \cdot \frac{V_D + V_O}{L} \cdot \frac{T_2}{T} \left(\frac{T}{2} - 2\Delta T \right) \quad (4)$$

Equations (3) and (4) can be transformed to obtain explicit relations for V_O and ΔT . From (3) we have:

$$\Delta T = \frac{1}{2} \cdot \left[T_2 - \left(\frac{T}{2} - T_2 \right) \frac{V_D - V_O}{V_D + V_O} \right] \quad (5)$$

Substituting ΔT in (4) and rearranging yields:

$$\frac{V_O}{V_D} = 2 \cdot \frac{R_L}{L} \cdot \frac{T_2}{T} \left(\frac{T}{2} - T_2 \right) \quad (6)$$

The third equation is found from the diode reverse recovery. Since our simple PWL diode model contains only linear capacitances and a linear resistance (in contrast to exponentially nonlinear ones in real diodes), the analysis involves only a simple RC circuit. The junction capacitances of the non-conducting diodes are neglected, since they pass only a small current. The converter model comprises three RC circuits driven by a current source (inductor current), which changes linearly with time. Diode reverse recovery is determined by the charging and discharging of C_F , so we must analyse the $R_F C_F$ circuit of Fig. 13. Two intervals are involved, shown in Figs. 12(e) and (f): the first lasts for $T/2 - T_2$, when $di_L/dt = (V_D + V_O)/L$; the second lasts for T_2 , when $di_L/dt = (V_D - V_O)/L$.

Interval I: The diode is switched on at the beginning of the first interval when C_F is empty. For a period $T/2 - T_2$ the $R_F C_F$ circuit passes the inductor current, and the instantaneous

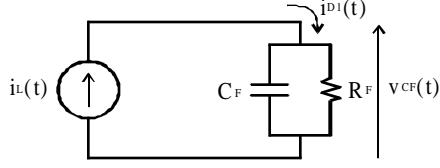


Fig. 13. Conducting diodes are driven by a linearly changing current source value of the charge q_{CF} on C_F is:

$$q_{CF}(t) = [q_{CF}(0^+) - q_{CFP}(0^+)] \exp(-t/\tau) + q_{CFP}(t)$$

where $q_{CF}(0^+) = 0$ is the initial charge immediately after the start of the interval ($t = 0$), $\tau = C_F R_F$ is the diode time constant (representing excess minority charge carrier recombination time) and q_{CFP} is the particular solution of the differential equation:

$$q_{CFP}(t) = \tau \cdot i_{D1}(t - \tau)$$

Since we neglect current through the junction capacitances C_j of non-conducting diodes, i_{D1} is nearly equal to i_L . Bearing in mind that:

$$i_{D1}(t) \approx i_L(t) = \frac{V_D - V_O}{L} t + \frac{V_D + V_O}{L} \Delta T$$

we obtain

$$q_{CFP}(t) = \tau \cdot \left[\frac{V_D - V_O}{L} (t - \tau) + \frac{V_D + V_O}{L} \Delta T \right]$$

and

$$q_{CFP}(0^+) = \tau \left(-\frac{V_D - V_O}{L} \tau + \frac{V_D + V_O}{L} \Delta T \right)$$

Finally, we get the instantaneous diode charge as

$$q_{CF}(t) = \frac{\tau}{L} \left\{ [(V_D - V_O)\tau - (V_D + V_O)\Delta T] \exp(-t/\tau) + (V_D - V_O)(t - \tau) + (V_D + V_O)\Delta T \right\}$$

At the end of this interval ($t = T/2 - T_2$), the charge on C_F is:

$$Q_{CF1} \frac{L}{\tau} = [(V_D - V_O)\tau - (V_D + V_O)\Delta T] \exp\left[-\left(\frac{T}{2} - T_2\right)/\tau\right] + (V_D - V_O)\left(\frac{T}{2} - T_2 - \tau\right) + (V_D + V_O)\Delta T \quad (7a)$$

Interval II: Now, following the same procedure and using $q_{CF}(0^+) = Q_{CF1}$ as an initial condition, we have the following equations:

$$i_{D1}(t) \approx i_L(t) = -\frac{V_D + V_O}{L} t + \frac{V_D + V_O}{L} T_1$$

$$q_{CFP}(t) = \tau \left[-\frac{V_D + V_O}{L} (t - \tau) + \frac{V_D + V_O}{L} T_1 \right]$$

$$q_{CFP}(0^+) = \tau \left(\frac{V_D + V_O}{L} \right) (T_1 + \tau)$$

and finally:

$$q_{CF}(t) = \frac{\tau}{L} \left\{ \left[Q_{CF1} \frac{L}{\tau} - (V_D + V_O)(T_1 + \tau) \right] \exp(-t/\tau) - (V_D + V_O)(t - \tau) + (V_D + V_O)T_1 \right\}$$

At the end of the second interval ($t = T_2$) the capacitance C_F is completely discharged, $q_{CF}(t) = 0$, and the diode switches off. Substituting $T_2 - \Delta T$ for T_1 , the above equation becomes:

$$0 = \left[Q_{CF1} \frac{L}{\tau} - (V_D + V_O)(T_2 - \Delta T + \tau) \right] \exp(-T_2/\tau) - (V_D + V_O)(\Delta T - \tau) \quad (7b)$$

The system of equations (5), (6) and (7) can be normalized with respect to the drive voltage V_D and the diodes' excess minority carrier recombination lifetime τ (equal to $R_F C_F$ in the PWL diode model):

$$v = \tau \cdot \frac{R_L}{L} \cdot \frac{2t_2}{T_n} \left(\frac{T_n}{2} - t_2 \right) \quad (8)$$

$$\Delta t = \frac{1}{2} \cdot \left[t_2 - \left(\frac{T_n}{2} - t_2 \right) \frac{1-v}{1+v} \right] \quad (9)$$

$$0 = [B - (1+v)(t_2 - \Delta t + 1)] \exp(-t_2) - (1+v)(\Delta t - 1) \quad (10a)$$

where

$$B = [(1-v) - (1+v)\Delta t] \exp\left(-\frac{T_n}{2} + t_2\right) + (1-v) \left(\frac{T_n}{2} - t_2 - 1 \right) + (1+v)\Delta t \quad (10b)$$

The normalized equations show that, out of eight circuit and diode parameters, only three qualitatively determine its behaviour: inductance L , load resistance R_L , and diode excess minority charge carrier recombination time $\tau \in$. All three appear in the first equation, forming a constant that can be denoted by a parameter $A \in \tau R_L / L$. This explains why the phenomenon can be observed experimentally even when fast diodes are used. If τ is small, the phenomenon appears at large R_L and/or small L . It appears at higher frequencies, since the drive period in equations is normalized by τ . For example, Fig. 3 was measured for $L = 9.42$ mH, $R_L = 10$ k Ω and $\tau = 7.2$ μ s, giving $A = 7.64$, and the maximum output voltage occurred at $f = 43$ kHz. Our model predicts a similar graph and behaviour with faster diodes having $\tau = 1$ μ s but with $L = 100$ μ H, $R_L = 764$ Ω . The maximum would then be at $f = 310$ kHz.

4. NUMERICAL SOLUTION

The nonlinear system of equations can be solved numerically, using the Newton-Raphson method (or similar). The results are shown in Figs. 14 through 17.

Fig. 14 shows how the normalized output voltage depends on the normalized drive period. Unlike the ideal case in Fig. 9, where the normalized output voltage is always less than unity and decays monotonically with rising frequency, here it is greater than unity, increases to a maximum, then decays more steeply toward zero. This agrees with the deviations noticed in practical converters, described above. The maximum value of the output voltage, and the frequency at which it occurs, depend on the parameter A . These functions, $v_{MAX} = f(A)$ and $f_{vMAX} = f(A)$, can be determined by calculating $\delta v / \delta A$ and are shown in Figs. 18 and 19.

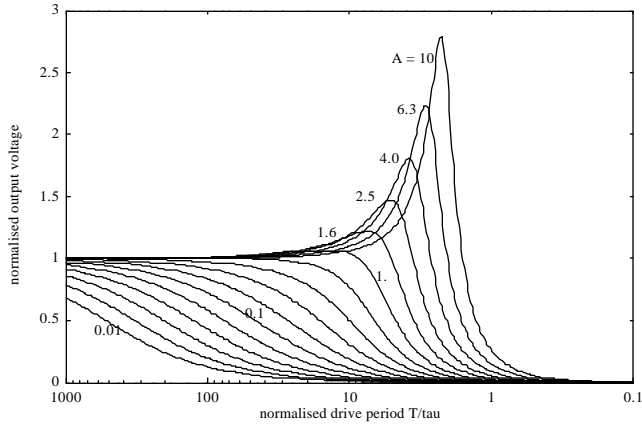


Fig. 14. Dependence of the normalized output voltage v on the normalized drive period T_n

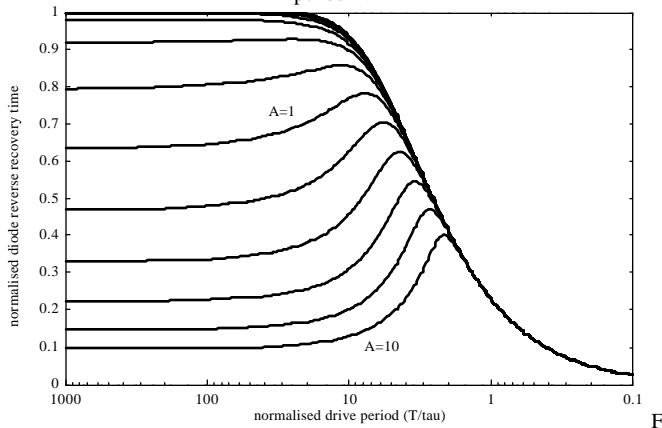


Fig. 15. Dependence of the normalized diode reverse-recovery time ΔT on the drive period T

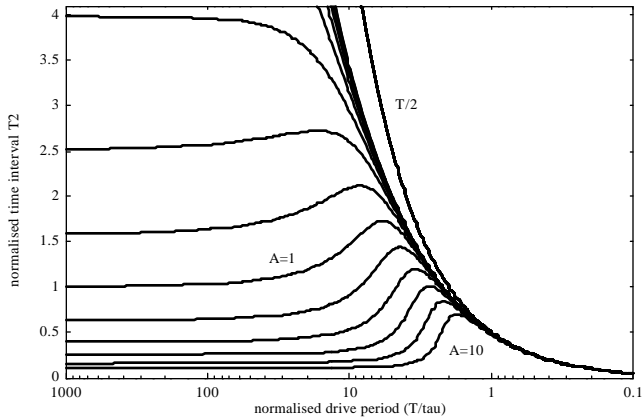


Fig. 16. Dependence of the normalized bridge pulses' delay time T_2 on the normalized drive period T_n

The numerical results are verified by comparison with experimental measurements. The experimental dependence shown in Fig. 6 was obtained for circuit parameters that give $A = 7.64$, and measurements give $v = 12.24/5 = 2.45$ and $T_n = 1/(43 \text{ kHz} \cdot 7.2 \text{ } \mu\text{s}) = 3.23$. The numerical results of Figs. 18 and 19 for the same A agree well: $v = 2.5$ and $T_n = 2.7$. This validates the simplifications made in the analysis.

Figs 15, 16 and 17 respectively show the dependence of the normalized diode reverse recovery time, the bridge pulse

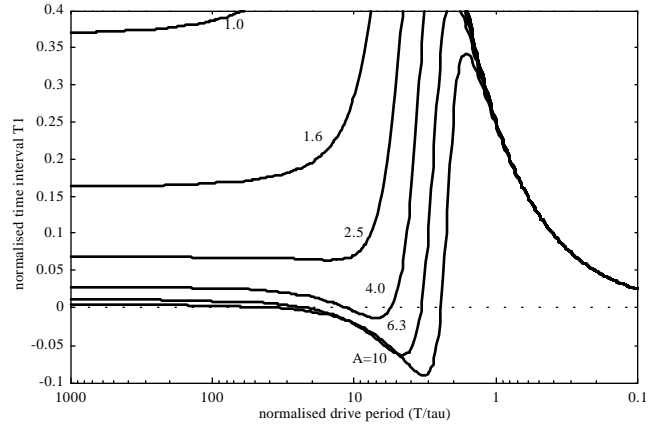


Fig. 17. Dependence of the normalized time interval T_1 on the normalized drive period T_n

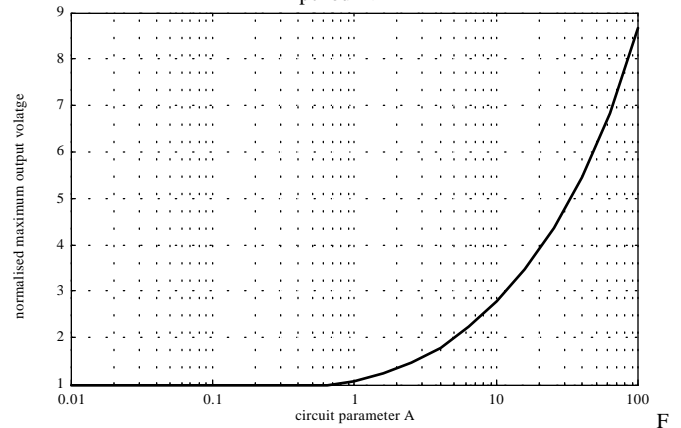


Fig. 18. Dependence of the maximum normalized output voltage on the parameter $A \in \epsilon \tau \epsilon R_i / L$

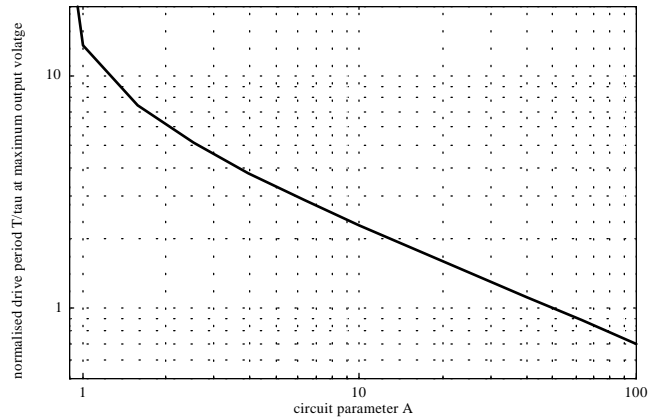


Fig. 19. Normalized drive period at maximum output voltage dependence on parameter $A \in \epsilon \tau \epsilon R_i / L$

delay, and T_1 on the normalized drive period. These dependencies are non-monotonic.

Moreover, since T_2 cannot increase further than $T/2$ when ΔT increases with V_o , T_1 becomes negative (see Fig. 17) for certain frequencies. This interval occurs at frequencies below those giving maximum voltage, and coincides with the appearance of the DH phenomenon. The two seem to be closely linked, and it is planned to investigate their connection in a future paper.

5. DESIGN CONSIDERATIONS

Figs. 14 and 18 show that the output voltage V_O becomes higher than the drive voltage V_D only when A becomes greater than unity (approximately). This overvoltage can be several times higher than V_D at higher A values, i.e. at light loads or with slow diodes, and might destroy output filter capacitors, usually designed for $V_O \leq V_D$. To avoid overvoltages and strange behaviour, the series-resonant converter and high-frequency rectifiers should be designed so that even in the worst case, i.e. at lightest loads, the condition $A = \tau R_L/L < 1$ is satisfied, giving $L/R_{L,MAX} > \tau$.

For example, the parameters used for Fig. 6 give the circuit time constant $L/R = 9.42 \text{ mH}/10\text{k}\Omega = 0.942 \mu\text{s}$, the diode time constant $\tau = 7.2 \mu\text{s}$ and $A = 7.2/0.942 = 7.64$. To make A less than unity we need to increase L/R , by decreasing R , increasing L , or adjusting both simultaneously.

If the circuit parameters are given, Fig. 14 and the above relation can be used to determine the maximum switching frequency above which the output voltage decreases below allowable limits, e.g. by 10% or less. (For this purpose, the voltage axis of Fig. 20 employs a log scale for improved legibility.) On the other hand, if the switching frequency is known, Fig. 20 gives the minimum A value for the same criterion. Hence the maximum allowable inductance at the input of the bridge rectifiers can be determined. This condition should be met even for the worse case, i.e. for the minimum value of R_L .

The above relation is also useful for the series-resonant converter, since at high frequencies its behaviour is similar (see Fig. 3 and 6). The relation should be added to the design rules for series-resonant converters [3, p. 405], and is a further reason for adding a pre-load at the output. Also, the correct frequency range for regulating the output voltage can be determined from Fig. 20.

6. CONCLUSION

Diode reverse recovery affects the operation of high-frequency rectifiers. The deviations from ideal operation can produce substantial overvoltages and quasi-periodic oscillations.

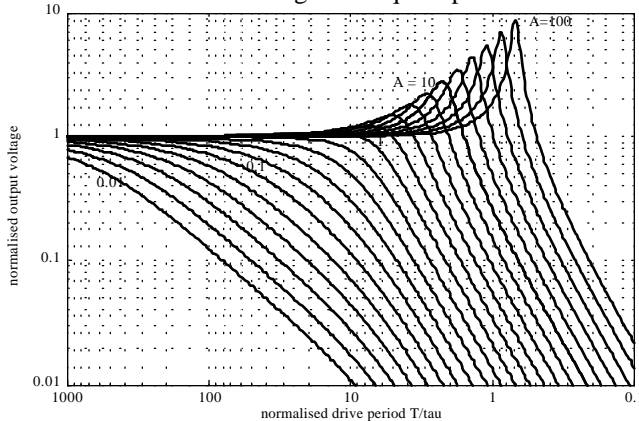


Fig. 20. Dependence of the normalized output voltage v on the normalized drive period T_n

tion, open-loop. The equations derived clearly show that the phenomena depend on $A = \tau R_L/L$, i.e. on only three out of eight circuit parameters. These are: (1) diode excess minority charge carrier recombination time; (2) converter load resistance; and (3) source inductance. Comparison with experimental measurements shows close agreement. When faster diodes are used, the same effects will be observed but at higher frequencies.

An additional constraint, $A < 1$ or $L/R_{L,MAX} > \tau$, should be added to the design rules for converters, in order to protect the circuit from overvoltages (which might damage output filter capacitors) and from open-loop instability (quasiperiodicity). For frequency-controlled converters, a modified frequency range should be used, and this can be determined from the graphs presented.

This work can form the basis for analysing similar phenomena in other converters. All switching converters have some stray inductance in series with their diodes, so we expect the phenomena to be widespread, especially as switching frequencies are pushed ever higher. Further investigations should explain the DH phenomenon and how it depends on circuit parameters; the general influence of delay; and similar effects in switching converters where the duty ratio is not 0.5. Analysis of appropriate control methods and their closed-loop stability are also of interest. These and other investigations are made possible now a suitable piecewise-linear diode model is available.

REFERENCES

- [1] Bimal K. Bose, "Power Electronics and Variable Frequency Drives: Technology and Applications", IEEE Press, IEEE Inc., New York, 1996.
- [2] Ned Mohan, Tore M. Underland and William P. Robins, "Power Electronics: Converters, Applications and Design", second edition, John Wiley & Sons, Inc., New York, 1995.
- [3] Marian K. Kazimierczuk and Dariusz Czarkowski, "Resonant Power Converters", A Wiley-Interscience Publishing, John Wiley & Sons, Inc., New York, 1995.
- [4] John G. Kassakian, Martin F. Schlecht and George C. Verghese, "Principles of Power Electronics", Addison-Wesley Publishing Company, Reading, Massachusetts, 1991.
- [5] Robert L. Steigerwald, "A Comparison of Half-Bridge Resonant Converter Topologies", IEEE Transaction on Power Electronics, Vol. 3, No. 2, pp. 174-182, April 1988.
- [6] Jonathan H.B. Deane and D.C. Hamill, "Instability, Subharmonics, and Chaos in Power Electronic Systems", IEEE Transactions on Power Electronics, Vol. 5, No. 3, pp. 260-268, July 1990.
- [7] Lupco V. Karadzinov, Goce L. Arsov and Ljupco Kocarev, "Amplitude Modulation Phenomenon in Series-Resonant Converters", 4th theme ETAI Symposium with international participation, pp. 33-34, Ohrid, Macedonia, September 27-29th, 1993, pre-print of synopsis papers.
- [8] Lupco V. Karadzinov, D.J. Jefferies, G.L. Arsov and J.H.B. Deane, "Simple Piecewise-Linear Diode Model For Transient behaviour", International Journal of Electronics, 1995, Vol. 78, No. 1, pp. 143-160.
- [9] Goce L. Arsov and Lupco V. Karadzinov, "Influence of the Circuit Parameters on the DH Phenomenon in Series-Resonant Converters", 8th Symposium Energetska Elektronika "Ee'95", Novi Sad, Yugoslavia, September 27-30th, 1995.